electrochem

MDPI

Article

Modification of Cu(111) Surface with Alkylphosphonic Acids in Aqueous and Ethanol Solution—An Experimental and Theoretical Study

Valbonë Mehmeti [1] and Fetah Podvorica [1,2,3,*]

[1] Department of Chemistry, FNMS, University of Prishtina "Hasan Prishtina", 10000 Prishtina, Kosovo; valbonamehmeti1@gmail.com
[2] Academy of Sciences and Arts of Kosova, 10000 Prishtina, Kosovo
[3] NanoAlb Research Unit: Surface Modification of Materials with Nanometric Organic Layers Group, "Fan Noli" Square, 1001 Tirana, Albania
* Correspondence: fetah.podvorica@uni-pr.edu

Abstract: Alkylphosphonic acids are well known for their ability to form self-assembled monolayers on hydroxide surfaces. A crucial step to understanding fundamentally how these surfaces are created is the elucidation of the interaction process that leads to such interface creation. In this study, we employed electrochemical impedance spectroscopy (EIS), Monte Carlo and molecular dynamics to understand this process. The interaction with the Cu(111) surface of three different alkylphosphonic acids (hexyl-, octyl- and decylphosphonic acids) is evaluated in an aqueous acidic and in an ethanol solution by Monte Carlo and molecular dynamics simulations, while EIS measurements are used to put in evidence the impact of the layer made in ethanol on copper protection. Nyquist diagrams of copper samples modified with an alkylphosphonic monolayer showed a higher polarization resistance that mitigates the copper corrosion in an aqueous acid medium. The phase–frequency Bode plots had higher and broader phase maxima for a modified copper surface with phosphonic moieties, which confirmed the ability of this organic layer to prevent copper corrosion.

Keywords: surface modification; alkylphosphonic acids; EIS; Monte Carlo; molecular dynamics; corrosion

Citation: Mehmeti, V.; Podvorica, F. Modification of Cu(111) Surface with Alkylphosphonic Acids in Aqueous and Ethanol Solution—An Experimental and Theoretical Study. *Electrochem* **2022**, *3*, 58–69. https://doi.org/10.3390/electrochem3010004

Academic Editor: Masato Sone

Received: 18 November 2021
Accepted: 29 December 2021
Published: 16 January 2022

1. Introduction

Inorganic compounds such as chromate (CrO_4^{2-}) have been used for many purposes such as chrome plating, leather tanning, copy machine toner, etc. [1]. Chromic anodizing has been applied for a long time in the aerospace industry due to its ability to protect aluminum alloys with copper (AA2000) against corrosion and to improve paint adhesion on their surfaces. Molybdate (MoO_4^{2-}) ions have shown protection abilities against zinc and copper [2,3] corrosion in the presence of chloride ions and copper and mild steel corrosion in artificial sea water [4].

Nevertheless, Cr(VI) compounds are very toxic because they cause severe damage to the skin, respiratory and gastro-intestinal tract, liver, kidneys and immune system [1]. Molybdate ions are toxic for freshwater organisms [5], therefore, CrO_4^{2-}, MoO_4^{2-} ions have been banned for use as inhibitors because of the toxicity and environmental damage they create [6]. Thus, lower toxicity, eco-friendly and nontoxic organic moieties such as phosphonic acids are used as organic corrosion inhibitors [7–9]. In wet corrosion environments, organic compounds which have heteroatoms such as oxygen, nitrogen and phosphorus can exhibit excellent inhibition against the corrosion of coinage metals. The capacity for the prevention of surface metal damage is based on the ability of their heteroatoms to coordinate with the corroding metal atom through their electrons. Hence, active corrosion sites on the metal surface are blocked, thereby, mitigating the rates of

anodic and cathodic reactions which occur during the electrochemical process, preventing, in this way, the corrosion of the metals. The nature of the solvent plays an important role in the formation of such films. Thus, using suitable nonpolar solvents, the interaction between the phosphonic acid group and the hydrophilic substrate can be amplified, in which case the phosphonate monolayer is formed for a very short time [7,10,11]. Phosphonic acid monolayers have been used as effective inhibitors on various substrates: Al [12–15], Ti [16–19], Fe [20], Zn [21], Cu, mild steel, bronze [22] and even Ta and Nb in different media due to their ability to form a complex with metal ions and reduce the corrosion damage of these materials.

At room temperature, 1–30 mM of phosphonic acid provided up to 95 % inhibition efficiency against the corrosion of copper in 0.1 M H_2SO_4 aqueous solution. Considering the immense importance of copper in many industries (such as heat exchangers, electrical boards and circuits), its protection against acid corrosion using highly effective and benign corrosion inhibitors is paramount [10,23,24].

The alkyl chain of the different organic molecules that are used to modify material surfaces has an impact on the quality of the deposited layer [25]. For this purpose, in the present work, we investigate the efficiency of phosphonic acids (hexyl-, octyl- and decylphosphonic acids, Figure 1) as corrosion inhibitors for copper in 0.1 M H_2SO_4 solution at room temperature. Self-assembled monolayers (SAMs) of alkylphosphonics were prepared only in ethanol solution due to their low solubility in water. The barrier effect of the alkylphosphonic layers onto copper surface in aqueous sulfuric acid solution were tested by electrochemical impedance spectroscopy (EIS) while we applied computational methods to theoretically elucidate the inhibitor–substrate interaction on the atomic and molecular levels in water and ethanol solution.

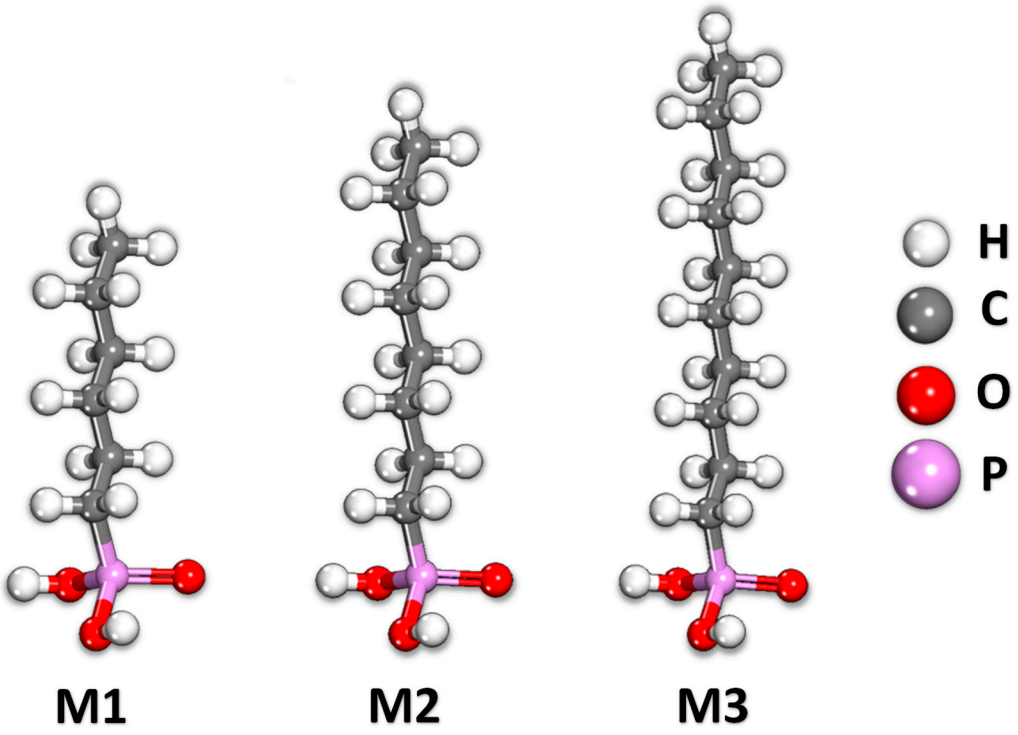

Figure 1. Structures of M1: hexylphosphonic acid, M2: octylphosphonic acid and M3: decylphosphonic acid used as in.

2. Methods and Computational Details

2.1. Chemicals and Electrodes

Hexylphosphonic acid 95%, octylphosphonic acid 97%, and decylphosphonic acid 97%, SIGMA-ALDRICH were used as inhibition molecules of corrosion. Sulfuric acid 97%,

pro analysis, MERCK, UN-No.1830 (Darmstadt, Germany) was used as the electrolyte for the EIS measurements. Its concentration in whole measurements was 0.1 mol/dm^3. All solutions were prepared from analytic grade chemicals and bidistilled water.

The copper electrode was made from a wire with diameter d = 2.2 mm. Prior to electrochemical measurements, metal surfaces were mechanically polished with emery paper, cleaned with distilled water and degreased in ethanol, washed with distilled water and finally dried in air. A saturated calomel electrode (SCE) and platinum electrode were used as reference and auxiliary electrodes, respectively.

2.2. Electrochemical Measurements

EIS measurements were performed using an Autolab potentiostat (Metrohm Autolab, Utrecht, The Netherlands) and employing a three-electrode cell assembly. This is a very sophisticated, fast and precise technique which helps to investigate the corrosion processes of a wide range of materials in certain corrosive environments. Information such as: surface properties, electrode kinetics and mechanical aspect can be obtained from impedance spectra [26–29]. The metal electrodes were allowed to stabilize their open circuit potential (OCP) until the potential stabilization criteria of dE/dt limit 10^{-6} V/s was reached. The initial applied frequency was 1×10^5 Hz, whereas finally frequency was 0.01 Hz. The points per decade were 7, whereas the amplitude was $\pm$10 mV.

2.3. Monte Carlo/Molecular Dynamics

In this study, we employed Monte Carlo and molecular dynamics to better understand at the molecular level the corrosion inhibition process. A Cu(111) model (periodic boundary conditions) with dimensions: 15.336 $\times$ 15.336 $\times$ 15. A vacuum layer at the C axis was used as a surface. The interaction with the Cu(111) surface of three different alkylphosphonic acids (hexyl-, octyl- and decylphosphonic acids) both in an aqueous acidic solution and an ethanol one was evaluated by Monte Carlo and molecular dynamics simulations [30–33]. The MD simulations with the Forcite Module (Materials Studio) were performed using COMPASS II [31–36]. Prior to the use of MD simulations, the surfaces were optimized using the Smart optimization algorithm with the energy convergence criteria of 10^{-4} kcal/mol and force criteria of 5×10^{-3} kcal/mol/Å.

3. Results and Discussion

Nyquist Plots

Nyquist plots obtained for the bare Cu electrode in aqueous H_2SO_4 0.1 M in the presence and the absence of phosphonic acids (hexyl-, octyl-, and decylphosphonic acids) are shown in Figure 2a–c. Alkylphosphonic monolayers on the Cu electrode surface were prepared by its immersion in ethanol 1 mM alkylphosphonic acid solution at different times (0.25, 1, 3, 6 and 24 h). The EIS results showed that all three alkylphosphonic SAMs on a copper surface had a much higher diameter of capacitive loop in the high frequency region (-Z" values: 4200, 6500 and 5000 Ω) than the 300 Ω of the bare Cu electrode. Their polarization resistance was increased due to the presence of the organic layer on the Cu surface that enabled the metal corrosion to be decreased, compared with the bare copper surface [37]. Almost all samples showed a straight line at low frequencies that was attributed to the diffusion of dissolved oxygen to the unmodified or modified copper surface [38,39].

The modulus–frequency Bode plots for the above shown EIS measurements are given in Figure 3 and they confirmed the increase in the impedance of all copper samples modified with alkylphosphonic layer compared to bare copper at the low frequency 0.01 Hz.

The phase–frequency Bode plots are also shown in Figure 3. The phase angle maxima for bare copper was 43° while it increased and became broader for the modified copper surfaces (65.5°; 67.5° and 65° for hexyl-; octyl-and decyl phosphonic layer, respectively). The broadening in the phase angle is due to surface coverage of the copper surface with alkylphosphonic layer. These results are in agreement with those obtained when a copper

surface was treated with amino acids: serine, cysteine and methionine in aqueous acid solution [39].

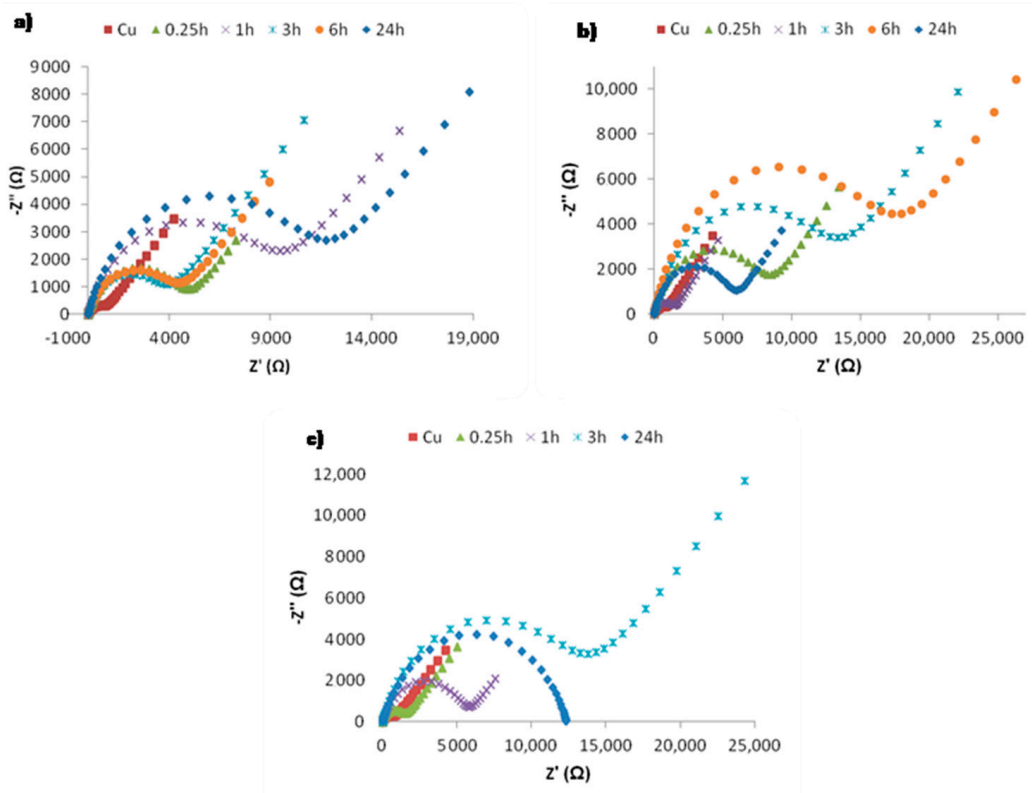

Figure 2. (**a**–**c**) Nyquist diagrams for Cu electrode in acid aqueous solution of H_2SO_4 0.1 M, unmodified and modified with self-assembled monolayer of (**a**) hexyl-, (**b**) octyl- and (**c**) decylphosphonic acids immersed in their solutions with concentration 1 mM in ethanol with different immersion times.

Corrosion inhibition in all cases (Table 1) was not dependent on the immersion time of the electrode in ethanol solution with a phosphonic acid concentration of 1 mM. The inhibition efficiency of using the phosphonic acids mentioned above in the case of a copper electrode was calculated by using the equation:

$$\% \, IE = \frac{R_p - R_0}{R_p} \times 100$$

where: *IE*—inhibition efficiency (%), R_p—polarization resistance of modified electrode, R_0—polarization resistance of unmodified electrode. Based on the results, it can be seen that such molecules are promising inhibitors by reaching up to 95% of corrosion inhibition.

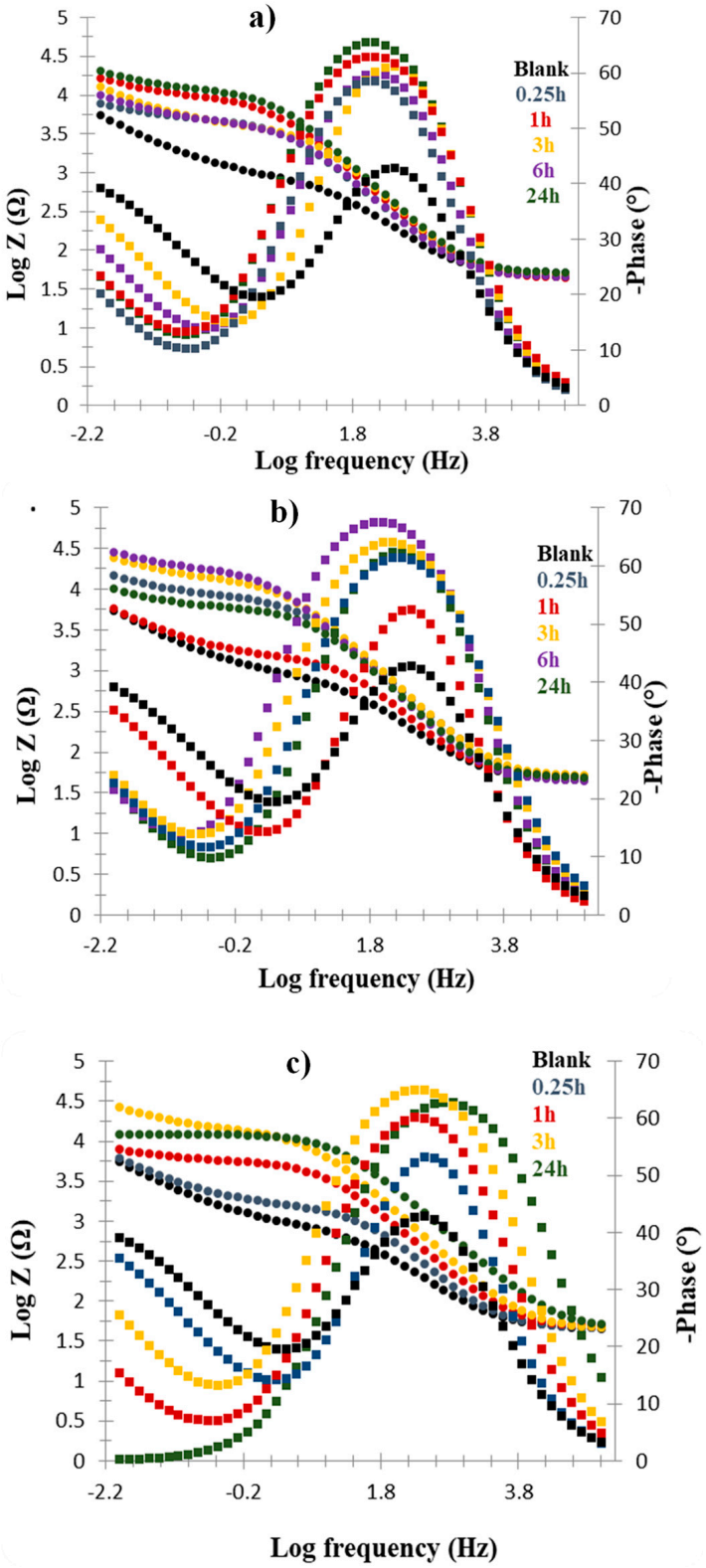

Figure 3. EIS data represented by Bode and phase angle variation vs. log frequency diagrams for Cu electrode in aqueous solution of H_2SO_4 0.1 M, unmodified and modified with self-assembled monolayer of (**a**) hexyl-, (**b**) octyl-, and (**c**) decylphosphonic acids immersed in their solutions with concentration 1 mM in ethanol with different immersion times.

Table 1. The values of polarization resistance and inhibition efficiency of corrosion at Cu electrode modified with phosphonic acids.

Cu/Molecule	R_s (Ω)	Q (Ω)	N	R_{ct} (Ω)	%*IE*
Blank	44.32	2.95×10^5	0.70	835.64	
Hexylphosphonic acid	50.55	6.3×10^6	0.8	11071	92.4
Octylphosphonic acid	44	6.87×10^6	0.81	16655	95
Decylphosphonic acid	44.67	2.558×10^6	0.76	12320	93.2

Equivalent electric circuit model or the so-called Randles circuit [23,24] used for fitting of experimental impedance data is given in Figure 4, where:

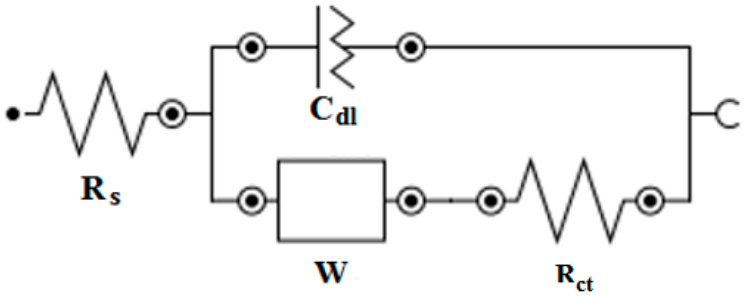

Figure 4. Equivalent electrical circuit model where R_s—electrical resistance of electrolyte, C_{dl}—electrical double layer, R_{ct}—the resistance of the electrical transfer charge, W—Warburg impedance.

R_s—shows electrolyte resistance, C_{dl}—capacity of electric double layer or known as element constant phase which shows the behavior of a non-ideal interface of metal-electrolyte capacity, whereas W shows the Warburg impedance and R_{ct} shows the charge transfer resistance of the interface.

The following EIS, Figure 5, plot shows the fitting results of the data using the equivalent circuit provided in Figure 4.

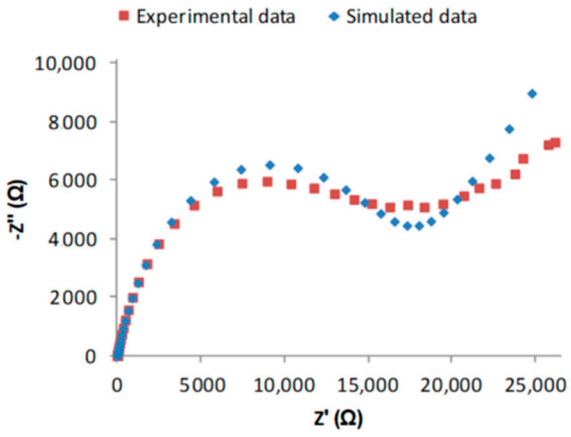

Figure 5. Nyquist plot of the data for Cu electrode in acid aqueous solution of H_2SO_4 0.1 M, modified with self-assembled monolayer of octylphosphonic acid (6 h) together with the fit resulting from the Randles circuit in Figure 4.

Furthermore, the Monte Carlo simulation enabled us to obtain the information about how the adsorption of the phosphonic molecules happens on the surface of the Cu (111) electrode in the aqueous sulfuric media (Figure 6) and in the presence of ethanol (Figure 7). The Monte Carlo results showed that these molecules were flat adsorbed onto the copper surface with the maximum adsorption energy of −72.4 kcal/mol (octylphosphonic acid). The same adsorption geometry (except for decyl phosphonic acid, which is perpendicu-

larly adsorbed) was observed also when the adsorption media consisted of ethanol (the adsorption energies were higher than in the previous adsorption media).

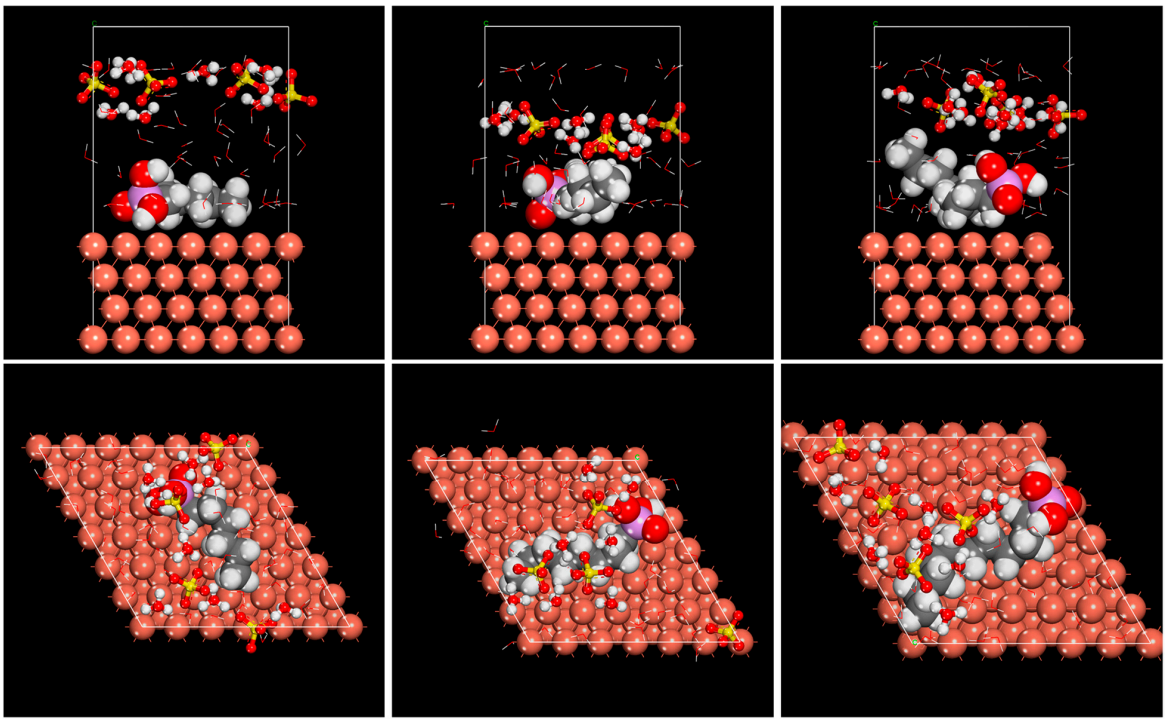

Figure 6. Top/side view of the equilibrium adsorption configuration of the alkyphosphonic acids' adsorption onto Cu(111) surface computed in aqueous acidic media (one alkylphosphonic acid + 47 water molecules + 8 hydronium ions + 4 sulphate ions) as obtained using the Monte Carlo simulation.

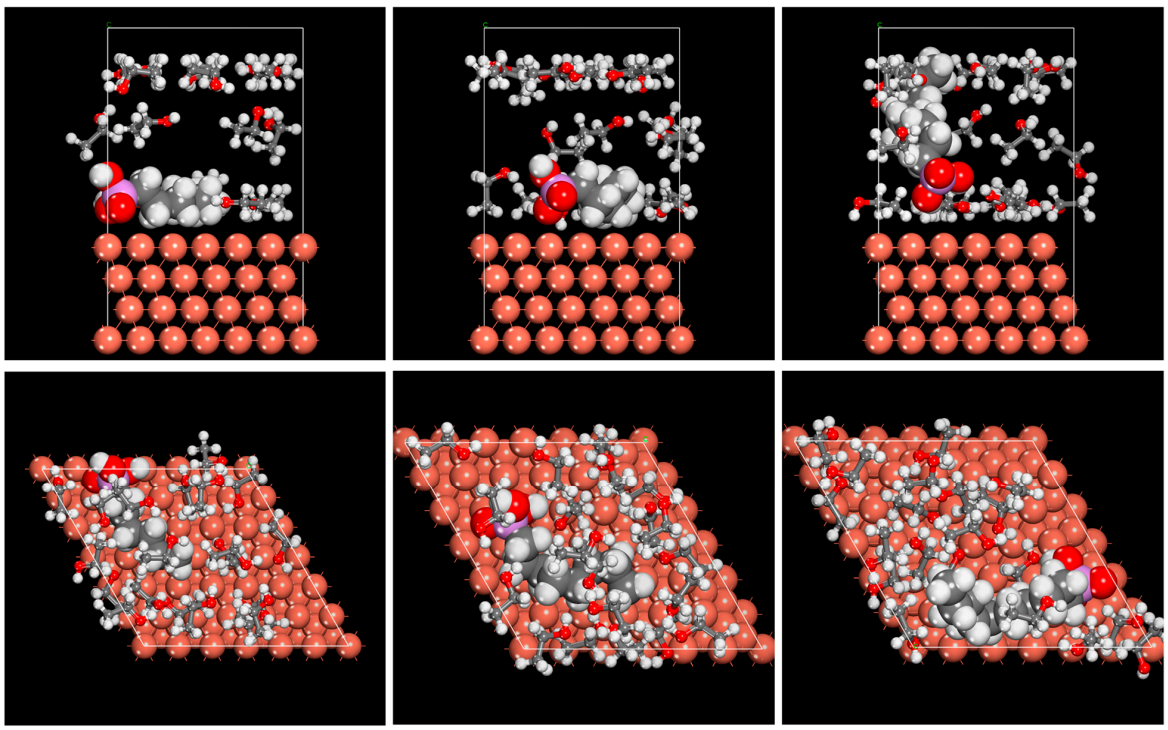

Figure 7. Top/side view of the equilibrium adsorption configuration of the alkyphosphonic acids' adsorption onto Cu(111) surface computed in ethanol (1 alkylphosphonic acid molecule + 20 ethanol molecule) as obtained using the Monte Carlo simulation.

The adsorption energy distributions of the alkylphosphonic acids on the Cu (111) surface was achieved by using the Monte Carlo calculations in aqueous and ethanol solution, as shown in Figures 8 and 9 and Table 2.

The MC results indicate that the adsorption interaction of the phosphonic carbon chain when this chain is shorter is more pronounced with the surface than the lateral interaction with other neighboring phosphonic acid molecules. When the alkyl chain is longer, the effect of lateral interaction is more pronounced and planar adsorption of the molecule prevails, therefore, it tends to be positioned toward the surface.

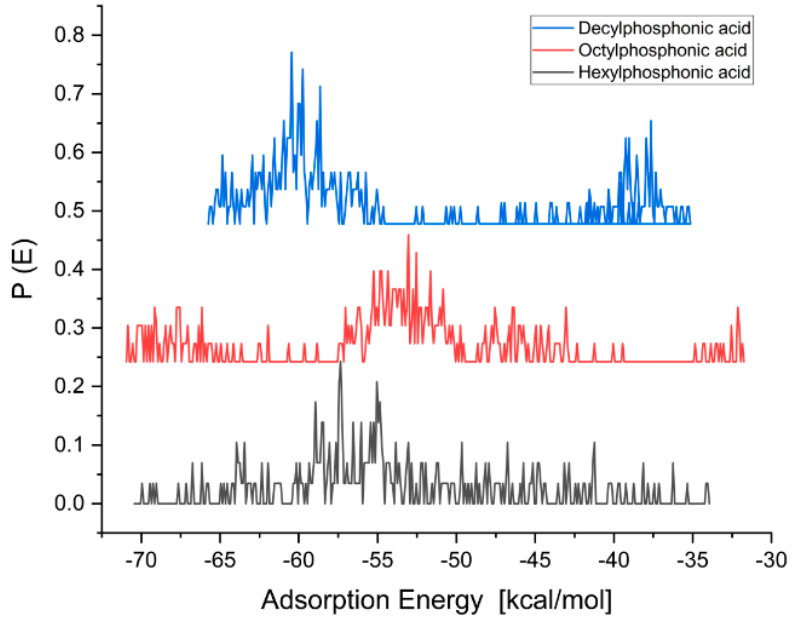

Figure 8. The adsorption energy of hexyl-, octyl- and decylphosphonic acids on the Cu (111) surface in aqueous medium.

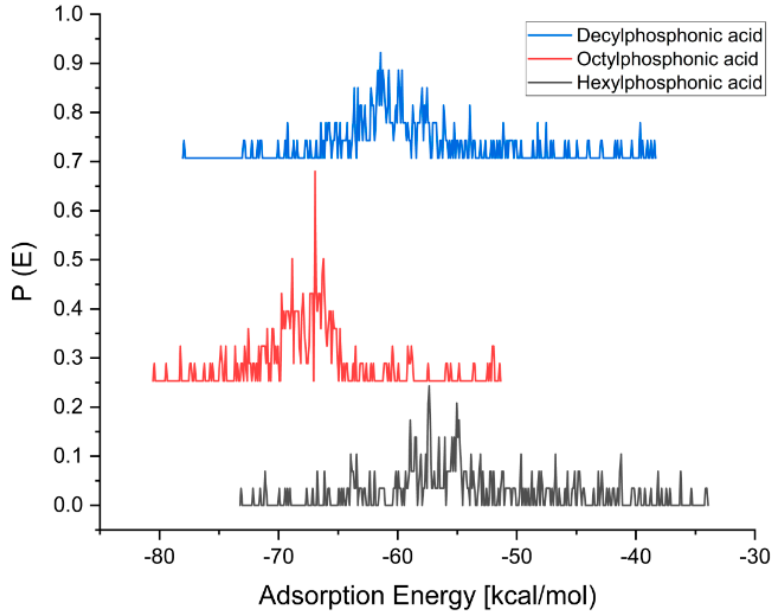

Figure 9. The adsorption energy of hexyl-, octyl- and decylphosphonic acids on the Cu (111) surface in ethanol medium.

Table 2. The adsorption energy of hexyl-, octyl-and decylphosphonic acids on the Cu (111) surface in aqueous medium and ethanol.

Molecule	Adsorption Energy [kcal/mol] (Water)	Adsorption Energy [kcal/mol] (Ethanol)
Hexylphosphonic acid	−71	−74
Octylphosphonic acid	−72	−82
Decylphosphonic acid	−67	−79

Although the MC can be used to evaluate the sorption properties of molecules onto the surface, MD is able to capture the dynamics of the adsorption process. The lowest energy configuration as obtained by MD (Figure 10) provides evidence of the tilted adsorption configuration of the phosphonic acids onto the copper surface with the head group (phosphonic group) positioned on the surface.

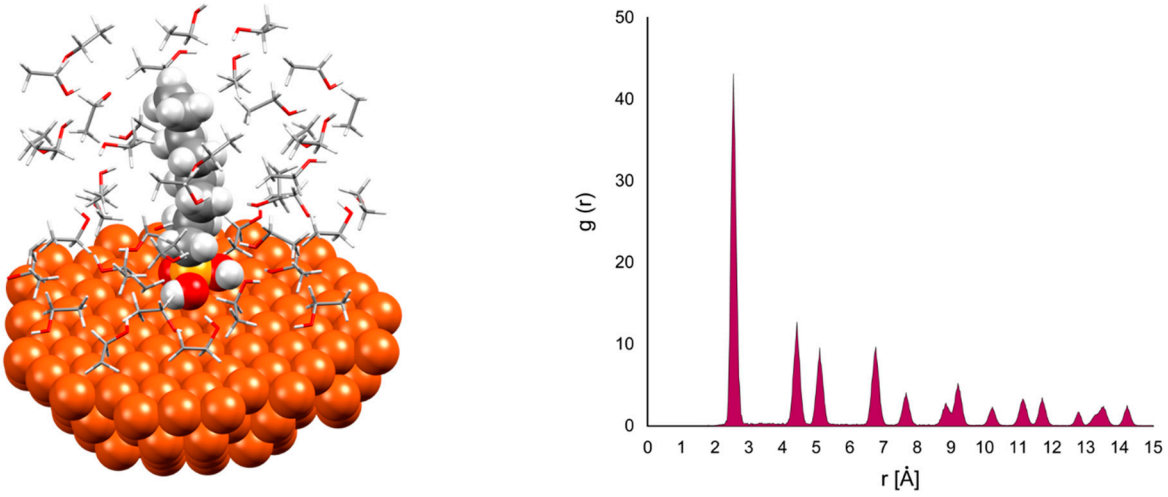

Figure 10. The final geometry of the MD simulation // forcefield = Condensed-phase Optimized Molecular Potentials for Atomistic Simulation Studies, NVT canonical ensemble at 298 K //. The time step for MD was 1 fs with a total simulation time of 500 ps, system temperature was maintained using a Berendsen Thermostat (0.1 ps decay constant). For the data analysis, 500 ps of trajectory frames were used.

The radial distribution function (RDF) presents a useful method to estimate the bond distances between the surface and the adsorbent. When the bond distances are in range from 1 Å up to 3.5 Å, this is indicative of chemisorption [40,41]. The RDF values of the alkylphosphonic acids in our MD simulations relative to Cu (111) surface as shown in Figure 10 are in the spike at 2.5 Å, supporting a chemisorption of these molecules onto the surface.

An indirect measure of the stability of the formed interface between the phosphonic acid and copper surface is the bond dissociation energy (BDE) [41–44]. The BDE values for the grafted phosphonic on the monohydroxylated icosahedral 13-atom copper cluster ranged between 32.53 and 39.46 kcal/mol. When compared to thiols, grafting phosphonic acids to the surface created more stable layers than thiol-derived self-assembling monolayers (SAM) [BDE | Au-S-$(CH_2)_5$-COOH | = 31.59 kcal/mol] [45] but is lower that of aryl groups on borophene [46].

4. Conclusions

The EIS results of the adsorption of phosphonic acids onto a copper (111) surface showed very good metal corrosion protection with an inhibition efficiency up to 95%.

The adsorption geometries and energies of the three alkylphosphonic acids on this substrate in the case of aqueous acidic media and ethanol were computed using Monte Carlo and molecular dynamics. The Monte Carlo results show that these molecules are flat adsorbed onto the copper surface with the maximum adsorption energy of −72.4 kcal/mol (octylphosphonic acid), the same adsorption geometry (except decylphosphonic acid which is perpendicularly adsorbed) is also observed when the adsorption media consist of ethanol (the adsorption energies are higher than in the previous adsorption media). The molecular dynamics calculations show that the orientation of the molecules with their head group (phosphonic acid) oriented perpendicularly toward the surface. The RDF curves (spikes at about 2.5 A) show a close distance interaction for all the alkyphosphonic acids with the Cu(111) surface.

Author Contributions: V.M.: literature review, methodology, resources, data curation, investigation, visualization, writing—original draft. F.P.: supervision, conceptualization, project administration, validation. All authors have read and agreed to the published version of the manuscript.

Funding: Please add: This research received no external funding.

Institutional Review Board Statement: Not applicable.

Informed Consent Statement: Not applicable.

Data Availability Statement: Data available in a publicly accessible repository.

Conflicts of Interest: Authors declare no conflict of interest.

References

1. Saha, R.; Nandi, R.; Saha, B. Sources and toxicity of hexavalent chromium. *J. Coord. Chem.* **2011**, *64*, 1782–1806. [CrossRef]
2. Aramaki, K. Effect of organic inhibitors on corrosion of zinc in an aerated 0.5 M NaCl solution. *Corros. Sci.* **2001**, *43*, 1985–2000. [CrossRef]
3. Shin, D.J.; Kim, Y.K.; Yoon, J.M.; Park, I.S. Discoloration resistance of electrolytic copper foil following 1,2,3-benzotriazole surface treatment with sodium molybdate. *Coatings* **2018**, *8*, 427. [CrossRef]
4. Sabet, B.K.; Dehghanian, C.; Yari, S. Corrosion inhibition of copper, mild steel and galvanically coupled copper-mild steel in artificial sea water in presence of 1H-benzotriazole, sodium molybdate and sodium phosphate. *Corros. Sci.* **2017**, *126*, 272–285. [CrossRef]
5. Heijerick, D.G.; Regoli, L.; Stubblefield, W. The chronic toxicity of molybdate to marine organisms. I. Generating reliable effects data. *Sci. Total Environ.* **2012**, *430*, 260–269. [CrossRef]
6. Muñoz, A.I.; Antón, J.G.; Guiñón, J.L.; Pérez Herranz, V. Comparison of inorganic inhibitors of copper, nickel and copper-nickels in aqueous lithium bromide solution. *Electrochim. Acta* **2004**, *50*, 957–966. [CrossRef]
7. Karthik, B.B.; Selvakumar, P.; Thangavelu, C. Phosphonic acids used as corrosion inhibitors-A review. *Asian J. Chem.* **2012**, *24*, 3303–3308.
8. Obot, I.B.; Onyeachu, I.B.; Wazzan, N.; Al-Amri, A.H. Theoretical and experimental investigation of two alkyl carboxylates as corrosion inhibitors for steel in acidic medium. *J. Mol. Liq.* **2019**, *279*, 190–207. [CrossRef]
9. Mehmeti, V.; Podvorica, F.I. Experimental and theoretical studies on corrosion inhibition of niobium and tantalum surfaces by carboxylated graphene oxide. *Materials* **2018**, *11*, 893. [CrossRef]
10. Fateh, A.; Aliofkhazraei, M.; Rezvanian, A.R. Review of corrosive environments for copper and its corrosion inhibitors. *Arab. J. Chem.* **2020**, *13*, 481–544. [CrossRef]
11. Obot, I.B.; Obi-Egbedi, N.O. Theoretical study of benzimidazole and its derivatives and their potential activity as corrosion inhibitors. *Corros. Sci.* **2010**, *52*, 657–660. [CrossRef]
12. Luschtinetz, R.; Oliveira, A.F.; Frenzel, J.; Joswig, J.-O.; Seifert, G.; Duarte, H.A. Adsorption of phosphonic and ethylphosphonic acid on aluminum oxide surfaces. *Surf. Sci.* **2008**, *602*, 1347–1359. [CrossRef]
13. Pellerite, M.J.; Dunbar, T.D.; Boardman, L.D.; Wood, E.J. Effects of Fluorination on Self-Assembled Monolayer Formation from Alkanephosphonic Acids on Aluminum: Kinetics and Structure. *J. Phys. Chem.* **2003**, *107*, 11726–11736. [CrossRef]
14. Messerschmidt, C.; Schwartz, D.K. Growth mechanisms of octadecylphosphonic acid self-assembled monolayers on sapphire (corundum): Evidence for a quasi-equilibrium triple point. *Langmuir* **2001**, *17*, 462–467. [CrossRef]
15. Bram, C.; Jung, C.; Stratmann, M. Self assembled molecular monolayers on oxidized inhomogeneous aluminum surfaces. *Fresenius. J. Anal. Chem.* **1997**, *358*, 108–111. [CrossRef]
16. Auernheimer, J.; Kessler, H. Benzylprotected aromatic phosphonic acids for anchoring peptides on titanium. *Bioorg. Med. Chem. Lett.* **2006**, *16*, 271–273. [CrossRef] [PubMed]

17. Danahy, M.P.; Avaltroni, M.J.; Midwood, K.S.; Schwarzbauer, J.E.; Schwartz, J. Self-assembled monolayers of α,ω-diphosphonic acids on Ti enable complete or spatially controlled surface derivatization. *Langmuir* **2004**, *20*, 5333–5337. [CrossRef] [PubMed]
18. Gawalt, E.S.; Avaltroni, M.J.; Danahy, M.P.; Silverman, B.M.; Hanson, E.L.; Midwood, K.S.; Schwarzbauer, J.E.; Schwartz, J. Bonding organics to Ti alloys: Facilitating human osteoblast attachment and spreading on surgical implant materials. *Langmuir* **2003**, *19*, 200–204. [CrossRef]
19. Gawalt, E.S.; Avaltroni, M.J.; Koch, N.; Schwartz, J. Self-assembly and bonding of alkanephosphonic acids on the native oxide surface of titanium. *Langmuir* **2001**, *17*, 5736–5738. [CrossRef]
20. Raman, A.; Dubey, M.; Gouzman, I.; Gawalt, E.S. Formation of self-assembled monolayers of alkylphosphonic acid on the native oxide surface of SS316L. *Langmuir* **2006**, *22*, 6469–6472. [CrossRef]
21. Montemor, M.F. Functional and smart coatings for corrosion protection: A review of recent advances. *Surf. Coat. Technol.* **2014**, *258*, 17–37. [CrossRef]
22. Van Alsten, J.G. Self-assembled monolayers on engineering metals: Structure, derivatization, and utility. *Langmuir* **1999**, *15*, 7605–7614. [CrossRef]
23. Amin, M.A.; Khaled, K.F. Copper corrosion inhibition in O_2-saturated H_2SO_4 solutions. *Corros. Sci.* **2010**, *52*, 1194–1204. [CrossRef]
24. Duran, B.; Bereket, G.; Duran, M. Electrochemical synthesis and characterization of poly(m-phenylenediamine) films on copper for corrosion protection. *Prog. Org. Coat.* **2012**, *73*, 162–168. [CrossRef]
25. Charlotte, M.S.; Mathieu, B.; Hélène, C.; Jaffrès, P.A. Phosphonic acid: Preparation and applications. *Beilstein J. Org. Chem.* **2017**, *13*, 2186–2213.
26. Randviir, E.P.; Banks, C.E. Electrochemical impedance spectroscopy: An overview of bioanalytical applications. *Anal. Methods* **2013**, *5*, 1098–1115. [CrossRef]
27. Nishikata, A.; Ichihara, Y.; Tsuru, T. Electrochemical impedance spectroscopy of metals covered with a thin electrolyte layer. *Electrochim. Acta* **1996**, *41*, 1057–1062. [CrossRef]
28. McIntyre, J.M.; Pham, H.Q. Electrochemical impedance spectroscopy; a tool for organic coatings optimizations. *Prog. Org. Coat.* **1996**, *27*, 201–207. [CrossRef]
29. Lasia, A. *Electrochemical Impedance Spectroscopy and Its Applications*; Springer: Boston, MA, USA, 2014; pp. 143–248.
30. Dagdag, O.; Berisha, A.; Safi, Z.; Dagdag, S.; Berrani, M.; Jodeh, S.; Verma, C.; Ebenso, E.E.; Wazzan, N.; El Harfi, A. Highly durable macromolecular epoxy resin as anticorrosive coating material for carbon steel in 3% NaCl: Computational supported experimental studies. *J. Appl. Polym. Sci.* **2020**, *137*. [CrossRef]
31. Dagdag, O.; Berisha, A.; Safi, Z.; Hamed, O.; Jodeh, S.; Verma, C.; Ebenso, E.E.; El Harfi, A. DGEBA-polyaminoamide as effective anti-corrosive material for 15CDV6 steel in NaCl medium: Computational and experimental studies. *J. Appl. Polym. Sci.* **2020**, *137*, 48402. [CrossRef]
32. Hsissou, R.; Benzidia, B.; Rehioui, M.; Berradi, M.; Berisha, A.; Assouag, M.; Hajjaji, N.; Elharfi, A. Anticorrosive property of hexafunctional epoxy polymer HGTMDAE for E24 carbon steel corrosion in 1.0 M HCl: Gravimetric, electrochemical, surface morphology and molecular dynamic simulations. *Polym. Bull.* **2019**, *77*, 3577–3601. [CrossRef]
33. Hsissou, R.; Benhiba, F.; Abbout, S.; Dagdag, O.; Benkhaya, S.; Berisha, A.; Erramli, H.; Elharfi, A. Trifunctional epoxy polymer as corrosion inhibition material for carbon steel in 1.0 M HCl: MD simulations, DFT and complexation computations. *Inorg. Chem. Commun.* **2020**, *115*, 107858. [CrossRef]
34. Hsissou, R.; Abbout, S.; Seghiri, R.; Rehioui, M.; Berisha, A.; Erramli, H.; Assouag, M.; Elharfi, A. Evaluation of corrosion inhibition performance of phosphorus polymer for carbon steel in [1 M] HCl: Computational studies (DFT, MC and MD simulations). *J. Mater. Res. Technol.* **2020**, *9*, 2691–2703. [CrossRef]
35. Benhiba, F.; Serrar, H.; Hsissou, R.; Guenbour, A.; Bellaouchou, A.; Tabyaoui, M.; Boukhris, S.; Oudda, H.; Warad, I.; Zarrouk, A. Tetrahydropyrimido-Triazepine derivatives as anti-corrosion additives for acid corrosion: Chemical, electrochemical, surface and theoretical studies. *Chem. Phys. Lett.* **2020**, *743*, 137181. [CrossRef]
36. Hsissou, R.; Benhiba, F.; Dagdag, O.; El Bouchti, M.; Nouneh, K.; Assouag, M.; Briche, S.; Zarrouk, A.; Elharfi, A. Development and potential performance of prepolymer in corrosion inhibition for carbon steel in 1.0 M HCl: Outlooks from experimental and computational investigations. *J. Colloid Interface Sci.* **2020**, *574*, 43–60. [CrossRef] [PubMed]
37. Qiang, Y.; Zhang, S.; Guo, L.; Zheng, X.; Xiang, B.; Chen, S. Experimental and theoretical studies of four allyl imidazolium-based ionic liquids as green inhibitors for copper corrosion in sulfuric acid. *Corros. Sci.* **2017**, *119*, 68–78. [CrossRef]
38. Zhang, D.Q.; Wu, H.; Gao, L.X. Synergistic inhibition effect of l-phenylalanine and rare earth Ce(IV) ion on the corrosion of copper in hydrochloric acid solution. *Mater. Chem. Phys.* **2012**, *133*, 981–986. [CrossRef]
39. Gong, Z.; Peng, S.; Huang, X.; Gao, L. Investigation the Corrosion Inhibition Effect of Itraconazole on Copper in H2SO4 at Different Temperatures: Combining Experimental and Theoretical Studies. *Materials* **2018**, *11*, 2107. [CrossRef] [PubMed]
40. Mendonça, G.L.F.; Costa, S.N.; Freire, V.N.; Casciano, P.N.S.; Correia, A.N.; de Lima-Neto, P. Understanding the corrosion inhibition of carbon steel and copper in sulphuric acid medium by amino acids using electrochemical techniques allied to molecular modelling methods. *Corros. Sci.* **2017**, *115*, 41–55. [CrossRef]
41. Hsissou, R.; Dagdag, O.; Abbout, S.; Benhiba, F.; Berradi, M.; El Bouchti, M.; Berisha, A.; Hajjaji, N.; Elharfi, A. Novel derivative epoxy resin TGETET as a corrosion inhibition of E24 carbon steel in 1.0 M HCl solution. Experimental and computational (DFT and MD simulations) methods. *J. Mol. Liq.* **2019**, *284*, 182–192.

42. Berisha, A. Interactions between the Aryldiazonium Cations and Graphene Oxide: A DFT Study. *J. Chem.* **2019**, *2019*, 5126071. [CrossRef]
43. Berisha, A. The influence of the grafted aryl groups on the solvation properties of the graphyne and graphdiyne-a MD study. *Open Chem.* **2019**, *17*, 703–710. [CrossRef]
44. Berisha, A.; Combellas, C.; Kanoufi, F.; Decorse, P.; Oturan, N.; Médard, J.; Seydou, M.; Maurel, F.; Pinson, J. Some Theoretical and Experimental Insights on the Mechanistic Routes Leading to the Spontaneous Grafting of Gold Surfaces by Diazonium Salts. *Langmuir* **2017**, *33*, 8730–8738. [CrossRef] [PubMed]
45. Berisha, A.; Combellas, C.; Kanoufi, F.; Médard, J.; Decorse, P.; Mangeney, C.; Kherbouche, I.; Seydou, M.; Maurel, F.; Pinson, J. Alkyl-Modified Gold Surfaces: Characterization of the Au-C Bond. *Langmuir* **2018**, *34*, 11264–11271. [CrossRef]
46. Berisha, A. First principles details into the grafting of aryl radicals onto the free-standing and borophene/Ag(1 1 1) surfaces. *Chem. Phys.* **2021**, *544*, 111124. [CrossRef]